

The science potential of ALFA: Adaptive optics with natural and laser guide stars

R.I. Davies¹, W. Hackenberg¹, T. Ott¹, A. Eckart¹, S. Rabien¹, S. Anders¹, S. Hippler², M. Kasper², P. Kalas², A. Quirrenbach³, and A. Glindemann⁴

¹ Max-Planck-Institut für extraterrestrische Physik, Postfach 1603, D-85740 Garching, Germany

² Max-Planck-Institut für Astronomie, Königstuhl 17, D-69117 Heidelberg, Germany

³ University of California, San Diego, Physics Dept., Center for Astrophysics & Space Sciences, Mail Code 0424, La Jolla, CA 92093-0424, U.S.A.

⁴ European Southern Observatory, Karl Schwarzschildstraße 2, D-85748, Garching, Germany

Received February 12; accepted May 25, 1999

Abstract. Adaptive optics with laser guide stars is mandatory in order to make use of the full capabilities of 8-m class telescopes. However, progress has been slow in two particular areas: techniques for spectroscopy at diffraction limited resolution and wavefront sensing on laser guide stars. ALFA – currently the only European laser guide star adaptive optics system, and the only one in the world open to guest observers – has made significant advances in both of these. In this paper we report on our first results from summer 1998, representing significant improvements over previous performance. We report on observations using natural guide stars which demonstrate that for bright stars ($m_V \lesssim 8$) ALFA can now reach K -band Strehl ratios in excess of 60% and easily resolve binaries at the diffraction limit of the telescope. We then present some of the first **integral field spectroscopy at diffraction limited scales**, showing we are able to distinguish spectra of binary stars with a separation of only $0.26''$. We also discuss results from a wide field image, which indicate that useful correction (allowing binary stars and circumstellar dust shells to be resolved) can be achieved from a relatively faint star to a radius of at least $1'$. Our last set of results include a **correction on a galaxy using the laser guide star** as the reference. The best result to date is of the galaxy UGC 1347 in Abell 262. Correcting tip-tilt on a star $41''$ away and higher orders on the laser, we achieved an increase in peak intensity of 2.5, and a reduction in FWHM from $1.07''$ to $0.40''$.

Key words: instrumentation: adaptive optics — instrumentation: laser guide stars — stars: binaries: close — stars: pre-main-sequence — galaxies: individual (UGC 1347)

1. Introduction

Adaptive optics for 8-m class telescopes is essential if their full potential is to be realised, and in order to achieve maximal sky coverage the use of laser guide stars is mandatory. Considerable effort has been put into developing high-order AO instrumentation and observational programmes: the number of refereed papers based on AO has been increasing dramatically (27 in 1997 compared to only 18 in the entire 4 years prior to that, Ridgway 1998), and recently an entire meeting was devoted to scientific results using adaptive optics systems (*Astronomy with Adaptive Optics*, ESO 1998). However, this also highlighted the fact that nearly all observations to date have been restricted to imaging studies, almost exclusively using natural guide stars as the wavefront reference. Further, the majority of results have been concerned with stellar systems and relatively few have been on extragalactic sources. This bias is simply a result of the lack of suitable reference stars since the most commonly observed extragalactic objects lie out of the galactic plane, while most bright stars lie in the galactic plane; and with the exception of a few of the brightest AGN, the nuclei of other galaxies are too faint for wavefront sensing with current technology.

Clearly, there is a need for development in the areas of artificial guide stars and diffraction-limited spectroscopy. But technical difficulties have slowed progress in producing high quality LGS, and practical difficulties have hindered advances in high spatial resolution spectroscopy. ALFA (Adaptive optics with a Laser For Astronomy, see Sect. 2) is addressing these issues and has made significant progress in both areas. In this paper we present some of our first observational results, which include these two areas. We begin by noting in Sect. 3 the best performance that ALFA has achieved, in context with other systems. In Sect. 4 the first spectroscopy at diffraction limited scales

is presented. Section 5 continues with observations of an $80'' \times 80''$ field around a Herbig Ae/Be star, looking at a binary, circumstellar envelopes, and the AO performance off-axis. The results from imaging a galaxy using the laser guide star as a wavefront reference are given in Sect. 6.

2. ALFA: An overview

ALFA is a sodium laser guide star (LGS) adaptive optics (AO) system installed at the Calar Alto 3.5-m telescope, and is currently available to guest observers. One major part of the system is a dye ring laser pumped by an Ar^+ laser, providing 3.8 W output at 589.2 nm with a bandwidth of 10 MHz (Quirrenbach et al. 1997). The laser is fed via a beam-relay to the launch telescope mounted beside the main mirror. Here a diagnostics bench (Rabien et al. 1998) provides an analysis of the beam quality before the laser is projected into the atmosphere. With good conditions the laser power is sufficient to produce a $m_V = 9$ mag artificial guide star by sodium fluorescence in the mesosphere at a height of 90 km. The adaptive optics bench is the other major component (Glindemann et al. 1997; Hippler et al. 1998; Wirth et al. 1998), and is based on a Shack-Hartmann wavefront sensor preceded by a set of hexagonal lenslet arrays which allow interchange between 6, 18, and 30 subapertures. A set of up to 32 Zernike modes or Karhunen-Loeve functions are derived and applied to a 97 actuator deformable mirror. While correcting on a natural guide star, the wavefront sensor can determine all modes including tip-tilt; when using a laser guide star, a separate tracker camera is used to measure the tip-tilt from a nearby star.

ALFA is the instrument on which a number of experiments have been carried out since 1998 in conjunction with the European network on *Laser Guide Stars for 8-m class Telescopes* (Foy 1999). These include determining tip-tilt from a LGS, monitoring the Na layer profile and scattered light, and simultaneous SCIDAR/ALFA measurements of atmospheric turbulence.

During the last 6 months significant progress has been made in the quality of correction that can be achieved with ALFA, even for mediocre atmospheric conditions. This is a necessity at the Calar Alto observatory since the seeing is often $1''$ or worse. For a number of observing programmes, ALFA is now able to compete effectively with other adaptive optics systems.

Some progress has also been made with the laser guide star, although this is still limited by non-ideal observing conditions, being particularly sensitive to atmospheric transmission. We have been able to close the loop on the laser and correct the field around the galaxy UGC 1347 with an improvement in both peak intensity and FWHM of a factor of 2.5. There remain two main restrictions to regular observations with the laser. One of these is the beam jitter, which can often throw the LGS spots outside

the centroiding regions on the wavefront sensor. The second is the LGS size ($\sim 2.5''$), the cause of which we are currently investigating; an intended fibre link to replace the beam relay between the laser and the telescope may overcome this. As well as these we are implementing automatic control algorithms for laser tuning and focussing, and also WFS focussing. These should increase the observing efficiency by a large margin.

Updates on progress with the system can be found online at http://www.mpe.mpg.de/www_ir/ALFA/ALFAindex.html.

3. Best performance

During 1998 the ALFA adaptive optics hardware and software underwent intensive optimisation and the system is now beginning to deliver the specified performances. These criteria include achieving 40% Strehl in the K -band with median $0.9''$ seeing.

For the purposes of this paper, Strehl ratios have been calculated from the ratio of peak to total fluxes in the PSF image, by comparing it to that calculated for the theoretical diffraction limited PSF (with a 3.50 m mirror and 1.37 m central obscuration). Unless stated, they take no account of where in the pixel the PSF is centred and hence may underestimate the actual Strehl. This error is rather variable: for example with $0.04''$ pixels a high Strehl measurement might be $50 \pm 5\%$, and with $0.08''$ pixels a lower Strehl measurement could be $15 \pm 5\%$.

For seeing of around $1''$, K -band Strehls in excess of 60% can be reached for the brightest stars ($m_V \lesssim 8$), while values in the range 25–50% can be attained for stars with $m_V \lesssim 10$. The performance achieved can be translated to other wavebands: we have achieved a J -band Strehl of 12% on SAO 56114 ($m_V = 7.0$) and a resolution better than $0.10''$, close to the diffraction limit of $0.07''$ FWHM. Previous efforts can be summarised by an observation in July 1997 of the $m_V = 5$ star 14 Peg for which we achieved K -band Strehl of only 20%, and so these new results represent a vast and speedy improvement, mainly due to upgrades in the hardware but also due to more careful alignment of the optical components and fine tuning of the modal reconstruction algorithms. Evidence for great advances in the field of AO generally can be found in the fact that such results are no more than is expected from other well established natural guide star systems such as *Pueo* (Rigaut et al. 1998), *ADONIS* (Le Mignant et al. 1999), and *Hokupa'a* (Close et al. 1999). However, it should be noted that operating in better seeing brings a huge benefit: a correction that results in a PSF with 25% Strehl in $1''$ seeing would achieve 40% Strehl in $0.7''$ seeing, which often occurs on Mauna Kea.

Even though the limiting magnitude is still lower than satisfactory ($m_V \sim 12$), the performance is very encouraging given that even if 32 (Zernike) modes are corrected *perfectly*, the residual wavefront error for the 3.5-m in $1''$

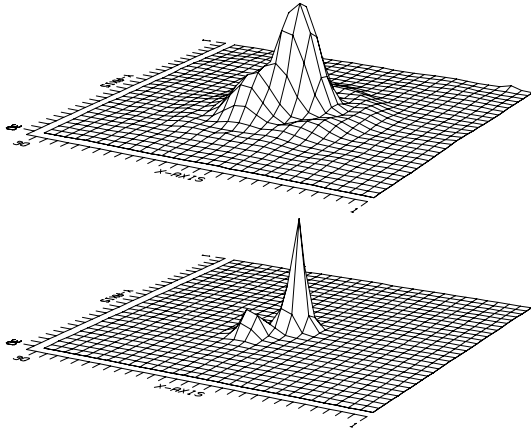


Fig. 1. *K*-band surface plots of SAO 36874 ($m_V = 5.9$), observed with a pixel scale of $0.04''$, and correcting 32 modes at a frame rate of 200 Hz. Upper: a direct image. Lower: a deconvolved image (30 iterations of the Lucy algorithm); the PSF star (SAO 56114, $m_V = 7.0$) had a Strehl ratio of 45% and a FWHM of $0.13''$. The two stars of SAO 36874 are clearly resolved at a separation of $0.15''$, only marginally greater than the *K*-band diffraction limit of the telescope

seeing in the *K*-band is $\sigma^2 = 0.43 \text{ rad}^2$ (Noll 1976) giving a maximum theoretical Strehl ratio of only 65%; and this does not include bandwidth limitations, noise, or other residual static aberrations – which are discussed below. The disturbance rejection bandwidth is typically 1/12 of the sampling frequency, while the temporal timescale of the atmosphere at $2 \mu\text{m}$ relates to a Greenwood frequency (Greenwood 1977) on the order of 10 Hz. Thus for frame rates of 300 Hz or more (e.g. for bright stars) the phase error due to bandwidth is small, while it becomes important at 100 Hz. The optimal frame rate requires minimising temporal errors and those from noise; a further parameter enters as we have several lenslet arrays available. The limiting magnitude is 1 – 2 mags brighter than that calculated from throughput and photon noise, much of which was due to faulty electronics in the Shack-Hartmann sensor and has been corrected for the 1999 semesters. The last additional input of errors is from static aberrations; most of these are removed by adjusting the deformable mirror shape until a reference fibre appears as a near-perfect PSF on the science camera.

One particular example of ALFA’s performance is the serendipitous discovery of a double star in SAO 36784 as shown in Fig. 1, during testing of control parameters. This star is listed in the Washington Double Star Catalog (WDS, Worley & Douglass 1997) as the primary partner of a pair with separation of $20.5''$ and magnitudes $m_V = 6.0$ and 12.3 . We have found that the primary itself is double, and almost certainly a true binary. Although we cannot rule out that it may be a projection effect, the probability of detecting *any* star (the cutoff is taken to be that the peak intensity of the companion is equal to the peak intensity of in the primary’s first airy ring) this close, given

the local stellar density, is $\sim 2 \cdot 10^{-8}$. The separation of the two components is $0.15''$, almost at the telescope’s diffraction limit ($0.13''$ FWHM), and they can clearly be discriminated after deconvolution. The observation shows the vast potential for studies of stars in multiple systems, for determining orbits and system stability, as well as for characterising spectroscopic and speckle binaries, by measuring broad-band colours or individual spectra. An example of the latter is given in the next section.

4. Integral field spectroscopy: HEI 7

The potential for spectroscopy at diffraction limited scales represents an exciting aspect of adaptive optics. However, the inherent difficulties also make it a special challenge. Standard techniques with a long slit may no longer be feasible, since in order to make the most of the benefits of minimising both background and contamination from extended sources, the slit must be extremely narrow. Accurately positioning a target on such a slit can be very time consuming, and for faint sources this becomes impractical. The alternative method of integral field spectroscopy which involves re-ordering a 2-dimensional field onto a longslit, dispersing it, and reconstructing a datacube (2 spatial and 1 spectral axes) afterwards, opens considerable opportunities in this area.

During August 1998, the MPE 3D imaging spectrometer (Weitzel et al. 1996), which obtains simultaneously *H*- or *K*-band spectra of an entire 16×16 pixel field, was used with ALFA. In order to facilitate this, an aperture interchange module (*AIM*, Anders et al. 1998) has been built as an interface to allow the pixel scale to be changed between $0.25''$ and $0.07''$ per pixel, as well as providing the ability for efficient sky observations with minimal overhead. Although the field of view is small ($1.2''$), this is ideally matched for observations of AGN or close binaries. Here we present some of the first spectroscopy at diffraction limited scales, of HEI 7, a binary listed in the WDS Catalog. The primary, more commonly known as HD 197443, is itself a photometric/spectroscopic binary (denoted AB) with a period of about 6 hrs and has not been resolved. A third member of the system (denoted C) was suspected from variations in the time of minimum in the primary pair, and its orbit was first calculated by Hershey (1975) from changes in parallax of the primary with respect to a set of reference stars (later confirmed by observation). The data yielded both the parameters of the AB-C 30.5 yr orbit as well as the absolute parallax, which sets the distance as 24 pc (ie the current projected separation is only 6 AU).

A PSF reference (HD 183051, left in Fig. 2) with the same $m_V = 7.1$ as the primary component of HEI 7 was observed 10 minutes before the binary using the same adaptive optics parameters. Although the first diffraction ring was complete when calibrating on the fibre at the beginning of the night, it is much more patchy in the stellar

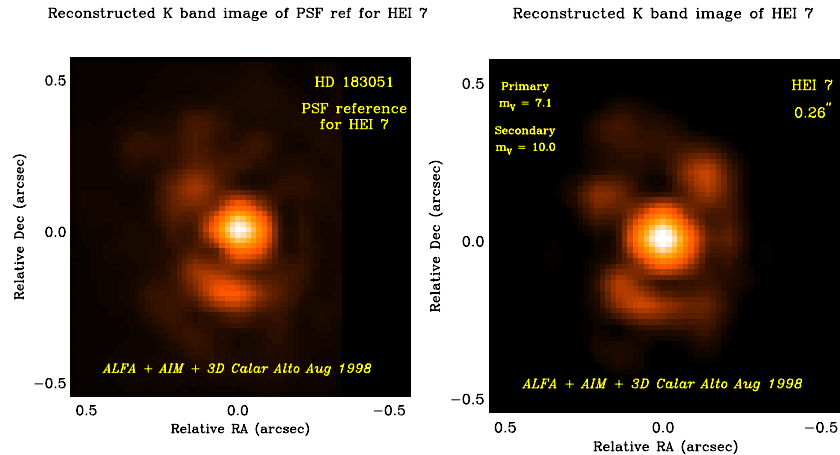


Fig. 2. Reconstructed K -band images of the PSF reference HD 183051 (left) and the binary HEI 7 (right), rebinned to a smaller pixel scale (original scale gives 16×16 pixels). North and East are rotated 15° from down and right respectively. Parts of the first diffraction ring can be seen; the extra blob to the top right in HEI 7 is the companion

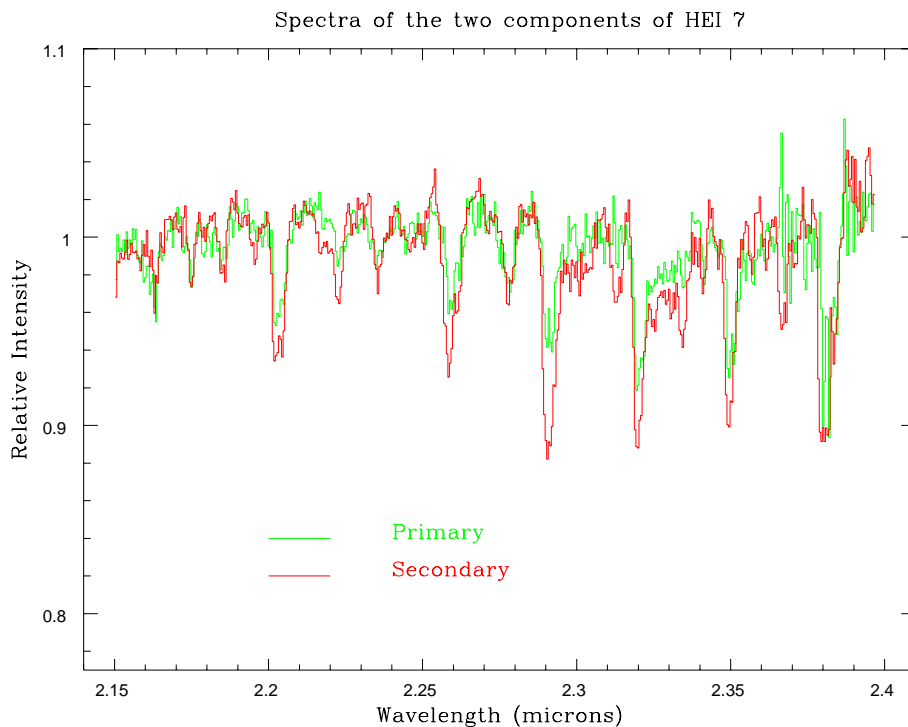


Fig. 3. Smoothed K -band spectra of the two components of HEI 7. All the features show the expected depth, based on spectral type classifications (K0 V and M0 V) of the two stars. In particular the ^{12}CO bandheads at 2.29, 2.32, 2.35, and 2.38 μm vary by almost a factor of 2, while the Mg line at 2.28 μm is the same for the two types. Other prominent lines include Na (2.21 μm) and Ca (2.26 μm)

image. Even so, the difference between this and the reconstructed K -band image of HEI 7 is clear: the secondary can be seen to the top right (south east) at a radial separation of 0.26'' and about a factor 15 fainter ($m_V = 10.0$).

Spectra of the two components are shown in Fig. 3. The primary (AB) component has the expected absorption features for a K0 V star; the differences between this and the secondary (C) are expected from its spectral type of M0 V (estimated from colours). In particular the ^{12}CO

bandheads are almost a factor of 2 deeper, while the Mg line has a similar equivalent width. The depth of the Na (2.21 μm) and Ca (2.26 μm) lines also shows some variation. These spectra, then, are from two separate objects and not simply the same one extracted at different points. This example clearly demonstrates the feasibility of diffraction limited spectroscopy, although the technique remains difficult. It is fortuitous that the diffraction ring is faint in the region near the secondary star so that

deconvolution is unnecessary. The next step is to develop methods which will allow overlapping spectra to be distinguished.

5. Wide field correction: BD +40° 4124

The 3D spectrometer was also used to obtain a K -band spectrum of the Herbig Ae/Be star BD +40° 4124 ($m_V = 10.6$, $m_K = 5.6$), while the field around this star was imaged in the JHK bands using Omega-Cass.

Herbig Ae/Be stars are the massive ($\gtrsim 3 M_\odot$) counterparts to the low mass T Tauri pre-main-sequence stars, typically being deeply embedded in gas and dust, but with strong hydrogen recombination lines. BD +40° 4124 lies in a small aggregate containing a few other similar stars (the nearest are another Herbig Ae/Be star V1686 Cyg, and the pair V1318 Cyg), but which is isolated from any large star-forming complex (Hillenbrand et al. 1995). Since it is by far the most massive (see Table 1) its effects on the local environment can be studied independently, and at a distance of marginally less than 1000 pc ($1'' \equiv 1000$ AU) adaptive optics can provide the resolution on solar-system scales which is required for studying the dust envelopes around these stars. As all the stars in the group have ages in the range $10^5 - 10^6$ yrs, this can be of some importance in understanding how massive stars are formed; and whether the winds, outflows, and radiation field around them influence the evolution of the aggregate.

The spectrum of BD +40° 4124 in Fig. 4 is remarkable in its lack of any features other than Brackett lines. The ratio of the lines $\text{Br}\gamma/\text{Br}\delta = 2.83$ suggests an extinction of $A_V = 29$ mag assuming an intrinsic ratio of 1.52 (case B, Osterbrock 1989) and either the $A_\lambda \propto \lambda^{-1.85}$ extinction law of Landini (1984) or the curves from Howarth (1983). This is rather higher than that given in Table 1 derived from optical lines, but is consistent with the $A_V = 45$ mag estimated via N_{H} from ^{12}CO and ^{13}CO luminosities (Hillenbrand et al. 1995). These observations can be reconciled if the line-emitting gas is mixed with the dust obscuring it, so that the optical lines sample only the surface regions and underestimate the extinction-corrected flux. However, the dust must then be internal to the H II region surrounding the star, and as much as 50 – 90% of the Lyman continuum photons would be absorbed before they could be processed into recombination lines (Wood & Churchwell 1989) reducing the recombination luminosity at all wavelengths. An alternative scenario is that the dust exhibits a dense clumpy structure so that the optical lines can sample the H II region through only the least-obscured lines-of-sight, the near-infrared lines denser regions, and the radio lines can probe through even the densest clumps.

For the wide field K -band image taken with Omega-Cass, BD +40° 4124 was centered in the wavefront sensor, allowing correction of 18 modes with a frame rate of 75 Hz. Although this star was saturated the Strehl ratios

and FWHMs of 14 others in the $80'' \times 80''$ field were measured, and these are plotted against their radial distance in Fig. 5. The FWHMs were estimated using only vertical and horizontal cuts (the “errorbars” are lines joining these points) since models suggest that the pixel size is already limiting the resolution: for Strehls of 10 – 15% an intrinsic resolution of $0.16''$ is expected, but the measurable resolution is $0.2 - 0.3''$ if the flux is binned into $0.08''$ pixels. The figure indicates that out to radii of at least $30''$, and perhaps even beyond, there is only a little degradation in performance. The isoplanatic angle (at zenith) θ_0 is taken to be the region over which the wavefront errors are identical, and a good approximation is given by Beckers (1993):

$$\theta_0 = 0.314r_0/H$$

where

$$H = \left(\int C_n^2 h^{5/3} dh / \int C_n^2 dh \right)^{3/5}$$

is an average distance to the turbulent layer (C_n^2 is the turbulence profile and r_0 is the coherence length). For infinite D/r_0 (D is telescope diameter) the wavefront errors due to anisoplanaticism reach 1 rad^2 at this radius (Humphreys et al. 1992), but for the 3.5-m at Calar Alto they are more typically 0.5 rad^2 . Thus for a perfect on-axis PSF, the strehl ratio will have fallen to 60%. Simple modelling following the prescription of Greenwood & Parenti (1994) shows that this effect should also be noticeable with a low on-axis strehl. An on-axis strehl of 15% should fall to 9% at a distance θ_0 off-axis and 6% at $2\theta_0$. A better understanding of why the isoplanatic patch appears so large can only be gained by studying the height and strength of the turbulent layers in the atmosphere, for example using SCIDAR to measure C_n^2 (Klückers et al. 1998), combined with analysis of the modal power spectrum determined from the measured gradients on the wavefront sensor, and the changes in the corrected off-axis PSF. We are carrying out such observations in collaboration with the TMR network and will present the results in a future paper. The SCIDAR results show that, as is always seen, there is a very strong boundary layer (Rigal & Wooder, private communication) at the telescope. At the 3.5-m this is a well-known problem due to difficulties controlling the mirror temperature, and would have the effect of widening the isoplanatic angle.

Due to the “core+halo” shape of the PSF, the effective resolution of only partially corrected images is better than that estimated using the FWHM. The diffraction limited core provides a strong contrast against the halo even if it contains only a small fraction (in this case about 12%) of the total flux. This is demonstrated in Fig. 6 which shows a star $20''$ from the reference has a clear sharp peak (as do all the single stars in the field), while another has a double peak, identifying it unambiguously as a previously unknown binary system with a separation of $0.32''$. Previous studies of multiplicity in Herbig Ae/Be stars (e.g.

Table 1. BD +40° 4124 region: stellar parameters

Star	Spectral Type	A_V /mag	$\log L/L_\odot$	M/M_\odot
BD +40° 4124	B2 Ve	3.6 – 3.8	4.10	13
V1686 Cyg	B5 Ve	4.2 – 6.7	2.77	4.5
V1318 Cyg North	mid A-Fe	7 – 15	–	> 1
V1318 Cyg South	mid A-Fe	8 – 15	–	> 1

All data from Hillenbrand et al. (1995).

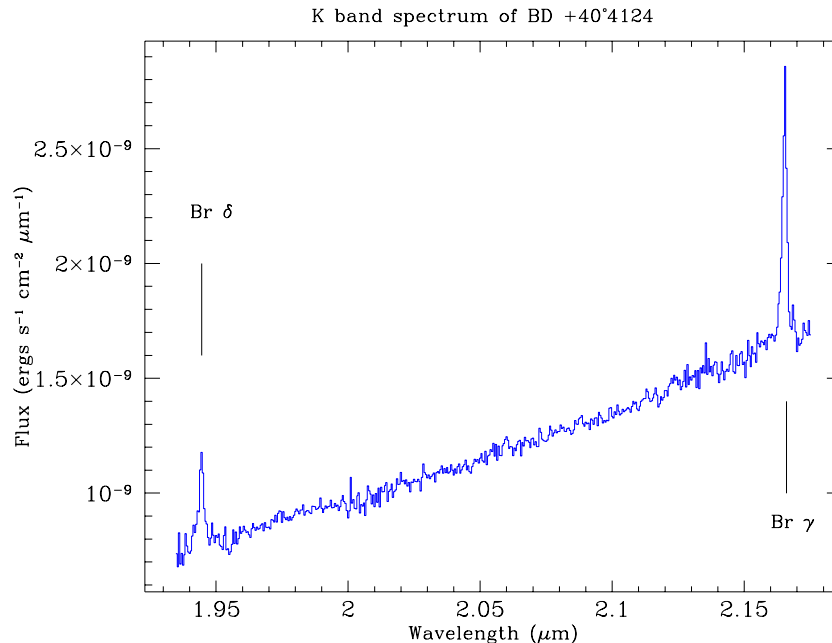


Fig. 4. *K*-band spectrum of BD +40° 4124. The continuum appears to be featureless except for the Brackett lines at 1.95 & 2.17 μm , suggesting an extinction of $A_V = 29$ mag

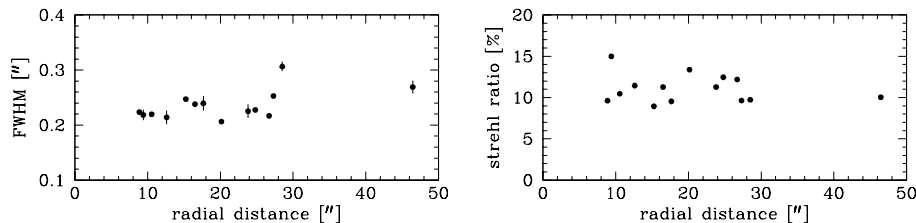


Fig. 5. Strehl ratio and FWHM of 14 stars in the field around BD +40° 4124, plotted against distance from this star. The advantage of working in the partial correction regime is clear, since the effects of anisoplanaticism are much reduced: only beyond 30'' is there a small reduction in performance

Leinert et al. 1997) have had to resort to speckle imaging, a slow and limiting process compared to adaptive optics. Importantly, examination of profiles of all the sources indicates that the speckle pattern in the halo appears to be stable over the whole field. Thus deconvolution should work well (yielding an effective resolution rather better than 0.2'') and the choice of PSF, at least in this case, is not critical. A further result from this image was that the southern star of the V1318 Cyg pair was resolved to be 0.4'' \times 0.3'', without the expected sharp core. The extinction to this object derived from the 1 – 0 Q(3)/1 – 0 S(1) ratio (Aspin et al. 1994) is $A_V = 45 \pm 20$ mag, us-

ing the same laws as above. Combined with very red *JHK* colours ($J - K = 4 - 5$ mag) this has led to interpretation as a dense circumstellar dust shell. We estimate the deconvolved size to be 300 \times 170 AU. Assuming the normal gas/dust ratio of 100, this is equivalent to $N_{\text{H}} = 7 \times 10^{22} \text{ cm}^{-2}$, and a gas density on the order of 10^6 cm^{-3} . At such densities vibrational levels of H_2 above $\nu = 1$ are collisionally de-excited, leading to large ratios between the $\nu = 1$ and higher levels whatever the excitation mechanism, for example 1 – 0 S(1)/2 – 1 S(1) > 10 (Aspin et al. 1994).

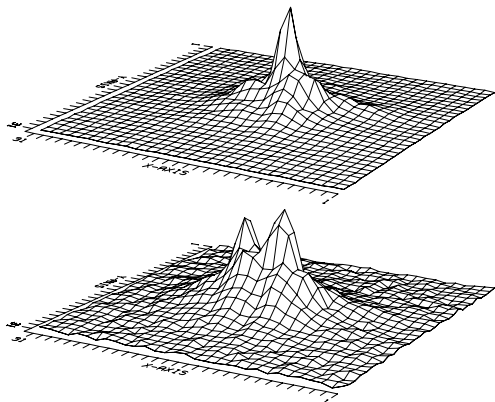


Fig. 6. *K*-band surface plots of a single star (upper) and the binary system (lower), both $\sim 20''$ from BD +40° 4124. The pixels are $0.08''$ across and the resolution is sufficient to easily separate stars $0.32''$ apart, as shown by the previously unknown binary system here. The profiles of all the stars show that the PSF changes very little out to distances beyond $30''$

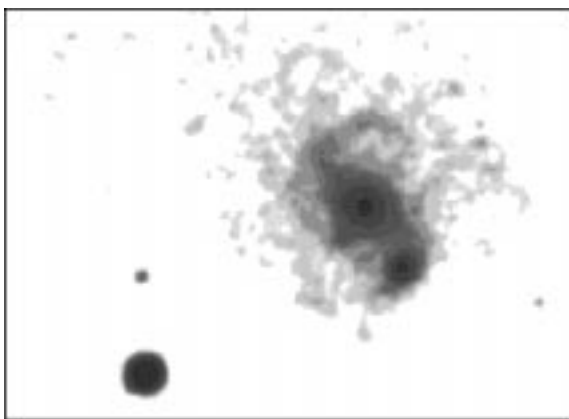


Fig. 7. Open loop *K*-band image of UGC 1347 (nucleus, and below it a compact H II region) and to the South-East the star used as the tip-tilt reference, smoothed to highlight the extended structure. The scale is given by the separation of the star from the galaxy nucleus of $41''$; North and East are up and left respectively

6. Laser guide star observations

The first successful wavefront correction using the LGS was on BD +31° 643, a binary star with separation $0.6''$, in December 1997, only 1 year after the first time the high-order adaptive optics loop was closed on any astronomical object. In August 1998 we used the LGS to correct the field around the galaxy UGC 1347 (Fig 7). For this observation we corrected tip-tilt using a $V = 11.8$ mag star $41''$ from the galaxy, and pointed the laser guide star midway between the two objects. High order corrections were measured using the LGS, with 6 subapertures sampled at a lower frame rate of 50 Hz (rejection bandwidth of only 4 Hz). Figures 8 and 9 show for the star an increase in peak intensity of 2.5, and improvement in resolution from $1.1''$ to $0.4''$.

There are only 2 other reported sodium laser guide star high-order corrections in the literature: at the MMT (Lloyd-Hart et al. 1998) and at the Lick Observatory (Olivier et al. 1996). Our correction is of a similar standard to these, and has an error budget dominated by approximately equal parts modal residual, isoplanatic and temporal, as well as noise. The noise is much higher than estimated by throughput and photon noise calculations, in part due to faulty electronics in the wavefront sensor which has now been replaced. This is the most likely reason for the asymmetric tail on the PSF, as it results in the centroid of the LGS spot being determined wrongly which leads to an incorrect modal decomposition. An additional source of noise arises from layers of water vapour high in the atmosphere. These scatter the laser beam, and sap the power from the LGS, resulting in low signal-to-noise and much poorer correction – this is perhaps the most serious difficulty at Calar Alto. One other problem we have had is that although the loop itself is stable, unpredictable low frequency (< 0.1 Hz) jitter in the upward laser beam can cause sudden glitches. This will be corrected for in future runs by feeding the jitter terms measured in the wavefront sensor back into the laser launch telescope.

6.1. Star formation in UGC 1347

Observations of UGC 1347 were carried out to look for centres of star formation in the galaxy, which can be identified by strong *K*-band emission from either a large population of red supergiant stars or hot dust around OB stars. In this galaxy there are 2 candidate sources: the nucleus and a region $11''$ from it at one end of the inner bar, probably an H II region. When the AO loop was closed, exactly similar enhancements were seen in both the star and the H II region, but almost no change is seen in the nucleus itself. The galaxy lies in the Abell 262 cluster at a distance of 63 Mpc, so $1''$ corresponds to 310 pc. Thus the LGS+AO corrected image shows that the nucleus is extended over 560 pc, a size similar to the bulges of spiral galaxies without a large population of young stars; contrarily the H II region is very compact – more typical of starbursts – with a diameter of much less than 130 pc (there is insufficient signal-to-noise to permit further deconvolution). Thus, although both regions have similar *K*-band luminosities, these observations suggest that all the current activity can be accounted for by the extra-nuclear region sited at one end of the inner bar.

7. Conclusion

We have presented an overview of recent results obtained with ALFA on the 3.5-m telescope at Calar Alto during the summer semester of 1998, which demonstrate the huge potential that this system has for science observations.

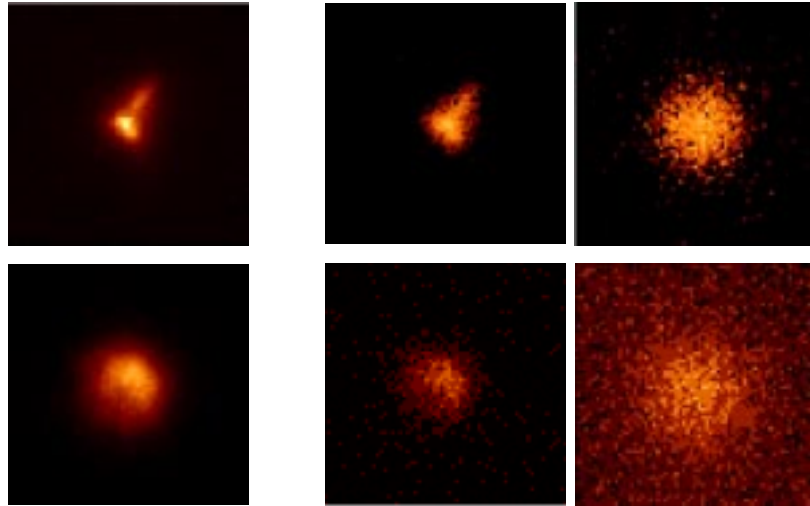


Fig. 8. Image sections $5.4''$ across corresponding to the profiles drawn below: of the tip-tilt star (left), and in UGC 1347 the compact H II region (centre) and nucleus (right); for both open loop (lower) and closed loop on the laser guide star (upper). Pixels are $0.08''$ across. The LGS-corrected PSF is not perfect but does show significant improvement beyond that achieved with tip-tilt alone

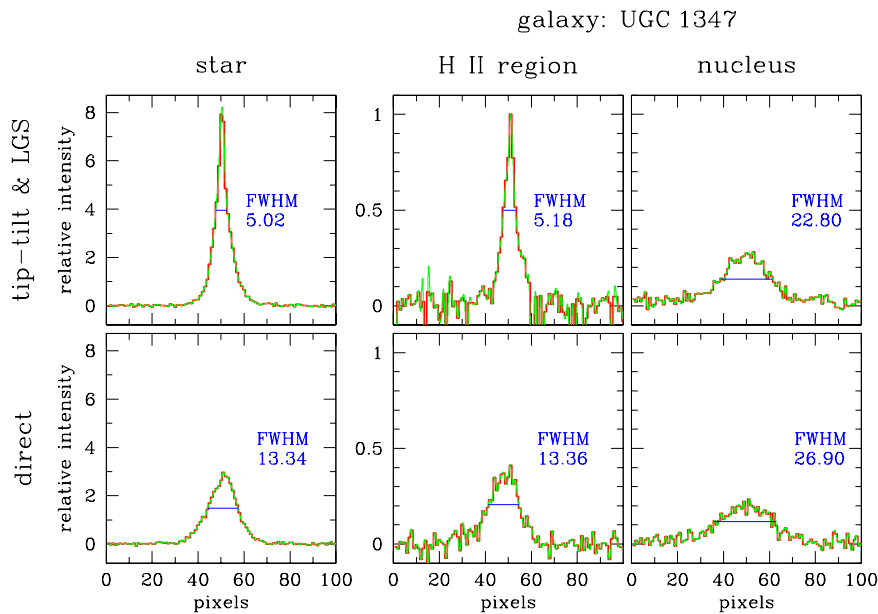


Fig. 9. Profiles of the star (left), and the compact H II region and nucleus of UGC 1347 (right) in both open loop (lower) and closed loop (upper). FWHM are given in pixels, with a scale of $0.08''$. The peak intensity of the star increases by a factor of 2.5, as does the unresolved H II region, while there is almost no enhancement in the nucleus showing it is completely resolved. The laser was used to correct the high orders in these images, while tip-tilt was determined from the star. Tip-tilt alone produced little improvement in image quality

The instruments most commonly used with ALFA are the MPE 3D integral field spectrometer and Omega-Cass (capable of imaging and polarimetry as well as long-slit spectroscopy). Using these we have achieved:

- excellent performance on bright stars yielding, in the K -band, diffraction limited resolution ($0.13''$) and high Strehl ratios (up to 60%),
- the first spectroscopy at diffraction limited scales, clearly distinguishing the spectra of both components

of the binary system HEI 7 at a projected separation of $0.26''$,

- spectroscopy of the Herbig Ae/Be star BD +40° 4124 and JHK images of an $80'' \times 80''$ field around it, resolving a binary system and a circumstellar dust envelope,
- a laser guide star corrected image of the galaxy UGC 1347 in the Abell 262 cluster which clearly highlights the difference between an unresolved compact H II region in the galaxy and its resolved nucleus.

ALFA is now beginning to show its true capabilities, and for some observing programmes is able to compete effectively with other adaptive optics systems. Observations with the laser guide star are still difficult, but improvements which will be implemented during early 1999 should stabilise closed loop operation and increase the observing efficiency.

Acknowledgements. The authors are grateful the Calar Alto staff for their help and hospitality. They also thank the rest of the ALFA team, as well as H.-C. Holstenberg, D. Looze, R.-R. Rohloff, K. Wagner, N. Wilnhammer, D. Hamilton, S. Beckwith, L. Appenzeller, and R. Genzel for their involvement in, hard work on, and enthusiasm for the project. Finally, thanks are due the camera teams for their efforts in maintaining and running 3D (MPE private instrument) and Omega-Cass (new instrument). RID acknowledges the support of the TMR (Training and Mobility of Researchers) programme as part of the European Network for Laser Guide Stars on 8-m Class Telescopes.

References

- Anders S., Maiolino R., Thatte N., Genzel R., 1998, in: *Infrared Astronomical Instrumentation*, SPIE, 3354
- Aspin C., Sandell G., Weintraub D., 1994, *A&A* 282, L25
- Beckers J., 1993, *ARAA* 31, 13
- Close L., Roddier F., Potter D., et al., 1999, in: *Adaptive Optics for Astronomy*, ESO
- Foy R., 1999, in: *Adaptive Optics for Astronomy*, ESO
- Glindemann A., Hamilton D., Hippler S., Rohloff R.-R., Wagner K., 1997, in: *Laser Technology for Laser Guide Star Adaptive Optics*, Hubin N., Friedmann H. (eds.), ESO, p. 120
- Greenwood D., 1977, *J. Opt. Soc. Am.* 67, 390
- Greenwood D., Parenti R., 1994, in: *Adaptive Optics for Astronomy*, Alloin D., Mariotti J.-M. (eds.), NATO ASI Conf., p. 185
- Hershey J., 1975, *AJ* 80, 662
- Hillenbrand L., Meyer M., Strom S., Skrutskie M., 1995, *AJ* 109, 280
- Hippler S., Glindemann A., Kasper M., et al., 1998, in *Adaptive Optics System Technologies*, Bonaccini D., Tyson R. (eds.), SPIE 3353, p. 44
- Howarth I., 1983, *MNRAS* 203, 301
- Humphreys R., Bradley L., Herrmann J., 1992, *Lincoln Lab. J.* 5, 45
- Klückers V., Wooder N., Nicholls T., et al., 1998, *A&AS* 130, 141
- Landini M., Natta A., Salinari P., Oliva E., Moorwood A., 1984, *A&A* 134, 284
- Leinert C., Richichi A., Haas M., 1997, *A&A* 318, 472
- Le Mignant D., Marchis F., Bonaccini D., et al., 1999, in: *Adaptive Optics for Astronomy*, ESO
- Lloyd-Hart M., Angel R., Groesbeck T., et al., 1998, *ApJ* 493, 950
- Noll R., 1976, *J. Opt. Soc. Am.* 66, 207
- Olivier S., Max C., An J., et al., 1996, *BAAS* 189, 42.08
- Osterbrock D., 1989, *Astrophysics of Gaseous Nebula and Active Galactic Nuclei*. University Science Books, Mill Valley, U.S.A.
- Quirrenbach A., Hackenberg W., Holstenberg H.-C., Wilnhammer N., 1997, in: *Adaptive Optics and Applications*, SPIE 3126, p. 35
- Rabien S., Hackenberg W., Ott T., Davies R., Eckart A., 1998, in: *Adaptive Optics for Astronomy*, ESO
- Ridgway S., 1998, in: *Adaptive Optical System Technology*, Bonaccini D., Tyson R. (eds.), SPIE 3353, p. 438
- Rigaut F., Salmon D., Arsenault R., et al., 1998, *PASP* 110, 152
- Weitzel L., Krabbe A., Kroker H., et al., 1996, *A&AS* 119, 531
- Wirth A., Navetta J., Looze D., et al., 1998, *Appl. Opt.* 32, 4586
- Wood D., Churchwell E., 1989, *ApJS* 69, 831
- Worley C., Douglass G., 1997, *A&AS* 125, 523